

Intrinsic Electrical Properties of Individual Single-Walled Carbon Nanotubes with Small Band Gaps

Chongwu Zhou, Jing Kong, and Hongjie Dai

Department of Chemistry and Laboratory for Advanced Materials, Stanford University, Stanford, California 94305

(Received 16 September 1999)

Individual single-walled carbon nanotubes (SWNT) exhibiting small band gaps on the order of 10 meV are observed for the first time in electron transport measurements. Transport through the valence or conduction band of a small-gap semiconducting SWNT (SGS-SWNT) can be tuned by a nearby gate voltage. Intrinsic electrical properties of the Ohmically contacted SGS-SWNT are elucidated. An SGS-SWNT exhibits metal- or semiconductorlike characteristics depending on the Fermi level position in the band structure.

PACS numbers: 72.80.Rj, 73.61.Wp

It is well established theoretically that the electronic structure of a single-walled carbon nanotube (SWNT) is remarkably sensitive to the nanotube chirality and diameter [1–6]. Band structure calculations have predicted that armchair SWNTs with (n, n) indices are truly metallic with finite density of states at the Fermi level, whereas SWNTs with (m, n) indices are semiconducting when $m - n \neq 3 \times \text{integer}$, and have primary energy gaps $E_g \propto 1/d$, where d is the nanotube diameter. SWNTs with (m, n) indices and $m - n = 3 \times \text{integer}$ are semimetallic with zero band gap within tight-binding calculations based on p_π orbitals alone. For this type of SWNT, Hamada *et al.* [3] and White *et al.* [4] have pointed out that the curvature of nanotubes leads to nonparallel p_π orbitals interacting with σ orbitals, which causes the opening of a small band gap to result in a semiconductor from a semimetal. Louie and co-workers have carried out first-principles *ab initio* calculations and found that the curvatures of small diameter SWNTs can lead to rehybridization of π^* and σ^* orbitals and thus altered electronic structures of SWNTs from those of flat graphene stripes [5]. Kane and Mele categorize SWNT into three types, truly metallic armchair SWNTs, semiconducting SWNTs (S-SWNTs), and curvature induced small-gap semiconducting (SGS) SWNTs [6]. For SGS-SWNTs, the band gaps depend on specific (m, n) indices and are in the range of 2–50 meV for $d = 3\text{--}0.7$ nm. For SGS-SWNTs with the same m/n ratio, the gap should scale as $1/d^2$ [6]. The small band gaps are expected to have nontrivial consequences to the electrical properties of SWNTs [5,6].

Electron transport [7–13] and scanning tunneling experiments [14,15] have identified individual metallic and semiconducting SWNTs. Thus far, measurements performed with individual nanotubes have not obtained evidence for the existence of small-gap semiconducting SWNTs. In transport studies, large metal-SWNT contact resistance has led to Coulomb charging effects [7,8] that obscure the intrinsic electrical properties of SWNTs [13]. This Letter reports the observation of individual semiconducting SWNTs with band gaps on the order of 10 meV.

Low metal-tube contact resistance enables the elucidation of the intrinsic electrical properties of the SGS-SWNTs.

Two terminal individual-SWNT devices were obtained by chemical vapor deposition growth of SWNTs from patterned catalyst islands on SiO_2 chips. Details of growth and device fabrication were given elsewhere [11,12,16]. We used 20 nm thick titanium (with 60 nm thick gold on top) as metal contacts. The lengths of the SWNTs between electrodes were typically $\geq 3 \mu\text{m}$. A degenerately doped silicon wafer with 500 nm thick thermally grown oxide on the surface was used as the substrate. The underlying conducting silicon wafer was used as a back gate. Figure 1 shows a tapping mode atomic force microscopy (AFM) image of an individual SWNT exhibiting small-gap semiconducting characteristics. The diameter of the SWNT was ~ 1.3 nm, determined by AFM topographic measurements. The current-voltage I - V curves obtained at room temperature are shown in Fig. 1. The linear I - V curve under zero gate voltage (V_g) showed a resistance of 36 k Ω . Increasing V_g reduced the conductance of the sample and reached a minimum at $V_g \sim 5$ V. A further increase in V_g led to conductance recovery, as seen in the conductance

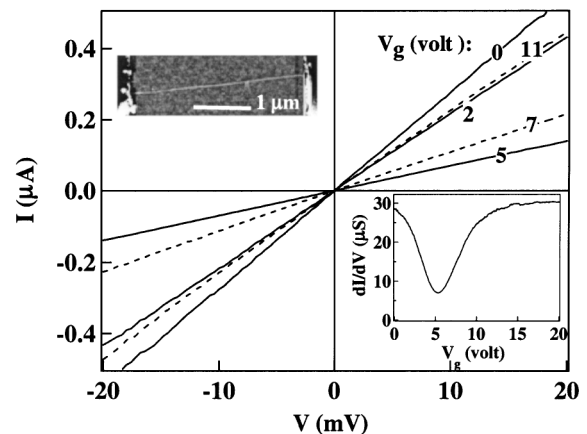


FIG. 1. Room temperature I - V characteristics of an SGS-SWNT. Bottom inset: dI/dV vs V_g . Top inset: AFM image of the $d \approx 1.3$ nm SWNT.

vs gate voltage curve (Fig. 1 inset) recorded under $V = 1$ mV. The conductance of the sample was suppressed by ~ 4 times at $V_g \sim 5$ V before the recovery, resulting in a valley in the conductance vs gate voltage curve.

We have recorded 400 I - V curves at 2 K in the bias range of $V = -40$ to 40 mV with $\Delta V = 400 \mu\text{V}$, under gate voltages in the range of $V_g = 0$ to 20 V with $\Delta V_g = 50$ mV. Figure 2(a) shows a grey-scale 2D conductance map obtained by plotting the conductance values at various (V, V_g) points. In the central region of the map within $V = -8$ mV to 8 mV and $V_g = 7.5$ to 10 V, the sample conductance is highly suppressed and the resistance is ~ 5 M Ω . However, the system is highly conducting in the corner regions where $|V| > 10$ –20 mV

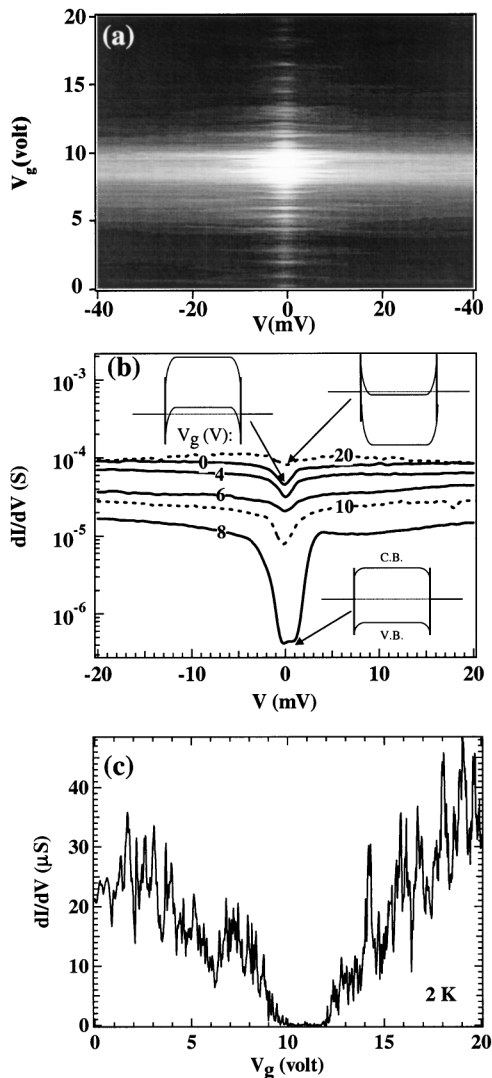


FIG. 2. (a) Grey-scale 2D conductance plot $\log(dI/dV)$ vs (V, V_g) recorded at 2 K. The brightest shade of grey corresponds to the lowest conductance $\sim 1 \times 10^{-7}$ S. The darkest shade corresponds to the highest conductance $\sim 4 \times 10^{-5}$ S. (b) dI/dV vs V curves recorded at various V_g . Inset: band diagrams under several gate voltages. (c) Zero-bias dI/dV vs V_g recorded at V_g^* .

and $V_g \sim 0$ or 20 V. The resistance in the corner regions is ~ 20 k Ω , more than 2 orders of magnitude lower than that in the central region. Figure 2(b) shows that as V_g increases from 0 to 8 V, the conductance vs bias voltage (dI/dV - V) curves shift downwards, but shift upwards upon a further increase in V_g . The I - V curves are non-linear near zero bias where dips of reduced conductance are observed. Under $V_g = V_g^* \sim 8$ V (V_g^* corresponds to the gate voltage under which the Fermi level of the nanotube is in the middle of the band gap), the conductance is highly suppressed for small biases $|V| < 8$ mV, as seen in the bottom curve in Fig. 2(b). The suppression is nearly exponential in V , indicating a gaplike structure in I - V . For gate voltages far away from V_g^* , only slight dips are seen in the dI/dV curves near $V = 0$ and the high bias conductance is $\sim 5 \times 10^{-5}$ S. We have also measured the zero-bias conductance dI/dV vs V_g using a lockin technique, as shown in Fig. 2(c). A gaplike region with highly suppressed conductance is observed between $V_g \sim 9$ to 12 V in the dI/dV - V_g curve. Outside the gap, the sample exhibits high conductance and some fluctuations.

The results presented above illustrate the small-gap semiconducting nature of the SWNT. Under V_g^* , the Fermi level of the nanotube is in the middle of the band gap. The physics of the system is similar to that of back-to-back Schottky diodes. Barriers exist to electrical transport at the metal-tube junctions, which leads to low conductance of the system. The low temperature data shown in the bottom curve in Fig. 2(b) suggests that the SWNT band gap is ~ 8 meV. For $V_g \ll V_g^*$, the Fermi level is inside the nanotube valence band and the system exhibits significant conductance since transport through the valence band can occur (p type). For $V_g \gg V_g^*$, the Fermi level is shifted into the conduction band, through which electron transport occurs (n type). The band gap can also be estimated from the conductance vs gate voltage data shown in Fig. 2(c), where the gap region exhibiting highly suppressed conductance spans $\Delta V_g \sim 3$ V. Using a gate efficiency factor $\alpha \sim 2.5$ mV/V [17], the band gap is estimated to be ~ 7.5 meV.

The low temperature data shown in Fig. 2 exhibit no clear signatures of Coulomb blockade. Thus, Coulomb charging effects are not dominant over the observed small-gap semiconducting characteristics. However, we do observe significant conductance fluctuations upon gate voltage variations, especially under low bias voltages ($|V| < 10$ mV), as streaking lines are seen near the central region in Fig. 2(a). These fluctuations could be due to electron interaction effects, but their precise origins are not understood at the present time. At 2 K, the resistance of the SWNT sample away from the central suppressed region in Fig. 2(a) is ~ 20 k Ω , which is close to the resistance quantum $h/2e^2$. The low resistance points to excellent metal-tube coupling, which is consistent with the fact that Coulomb charging is not the dominant phenomenon observed with the sample.

We have also elucidated the temperature dependent electrical properties of the small-gap semiconducting SWNT. The linear conductance vs gate voltage curves measured at 290, 60, and 10 K under $V = 1$ mV are shown in Fig. 3(a). It is observed that V_g^* drifts as the temperature is decreased. The drifts can be interpreted as due to changes in the electrostatic charge state of the substrate, as the temperature is lowered [18]. To correct for this unwanted effect, we determine the temperature dependent resistance of the SWNT sample under conditions with fixed Fermi-level position relative to the bands at all temperatures. At $V_g^*(T)$, the valley resistance is found to scale as $\exp(-E_a/K_B T)$ with $E_a \sim 6$ meV, as shown in Fig. 3(b). This suggests that when the Fermi level resides inside the band gap, transport through the SWNT under small bias voltages is thermally activated across a barrier $\sim E_g/2$. The small-gap semiconducting nature of the SWNT is thus fully manifested. On the other hand, under $V_g = V_g^*(T) - 5$ V, the resistance of the SWNT exhibits drastically different dependence on temperature as shown in the inset in Fig. 3(b). The resistance *decreases* from ~ 36 to 25 k Ω as temperature decreases from 290 to 80 K. At even lower temperatures, the I - V curve exhibits nonlinearity with suppressed conductance near $V = 0$, and the resistance increases with a decrease in temperature. These results show that, when the Fermi level resides within the valence (or conduc-

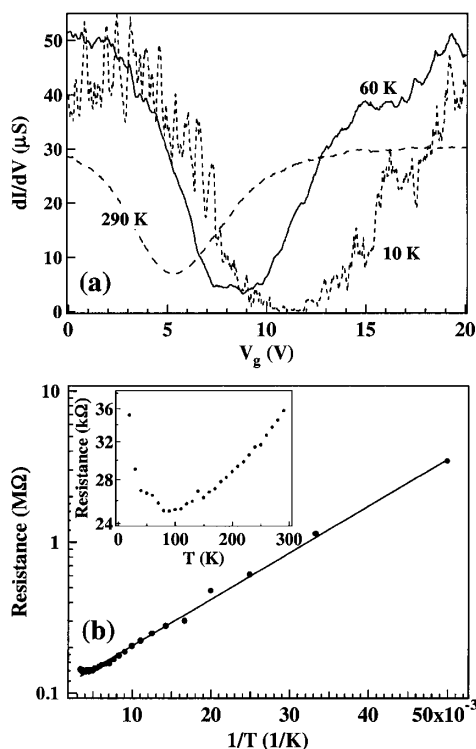


FIG. 3. (a) dI/dV vs V_g curves recorded at 290, 60, and 10 K, respectively. (b) Linear resistance vs $1/T$ measured under $V_g^*(T)$. Solid line: fitting of $R(T) \sim \exp(-E_a/K_B T)$ with $E_a \sim 6$ meV. Inset: Resistance vs T measured under $V_g^*(T) - 5$ V and a bias of $V = 1$ mV.

tion band, data not shown), the small-gap semiconducting SWNT sample behaves like a quasimetal. The positive slope in $dR(T)/dT$ for $T > 80$ K can be attributed to reduced phonon (e.g., twiston) scattering [6,19] as temperature decreases. The resistance upturn at lower temperatures could be due to small barriers existing at the metal-tube junctions due to band bending effects.

The origin of the observed small band gap could be attributed to the nontrivial curvature effects predicted to exist in small-diameter SWNTs [3–6]. The SWNT is not an S-SWNT with large primary band gap on the order of 600 meV expected for an S-SWNT with $d \sim 1.3$ nm. The transport characteristics of the SGS-SWNT differ significantly from S-SWNTs described in Refs. [9–13] and [20]. Out of ~ 20 systematically characterized individual SWNT samples so far, we observed three SWNTs exhibiting small-gap semiconducting behavior described above. The electrical properties of SGS-SWNTs can also be distinguished from metallic SWNTs. Figure 4 shows the results obtained with a different SWNT ($d \sim 2.2$ nm, length ~ 3 μm) that exhibited metallic characteristics. The resistance of this tube decreased from ~ 17.5 k Ω at 290 K to ~ 11.5 k Ω at 50 K. Below 50 K, the resistance curve made a slight upturn but remained below 12 k Ω . At 4 K, the dI/dV vs V curve exhibited a slight conductance suppression near $V = 0$ (Fig. 4 inset). Importantly, for various V_g in the range of -100 to 100 V, no well-defined region with diminished conductance was observed, suggesting that the SWNT was metallic with no detectable band gap. The zero-bias conductance suppression in this case could be due to electron-electron interaction effects, a phenomenon observed previously in metallic SWNT and multiwalled nanotubes at low temperatures [21,22]. Note that the lowest resistance measured with this 3 μm long tube was ~ 11.5 k Ω .

In summary, we have presented for the first time, the elucidation of the intrinsic electrical properties of individual small-gap semiconducting SWNTs. Excellent coupling

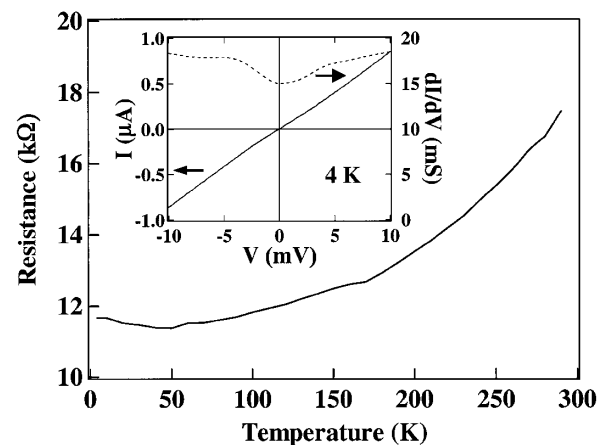


FIG. 4. Temperature dependent resistance of a metallic SWNT. Inset: I - V and dI/dV - V curves recorded at 4 K.

from metal electrodes to various types of SWNTs can be reproducibly obtained within our controlled fabrication approach, which leads to low contact resistance on the order of $h/2e^2$ and facilitates the investigation of transport properties of SWNTs.

This work was supported by NSF, DAPRA/ONR, SRC/Motorola, Stanford Center for Materials Research, the David and Lucile Packard Foundation, a Terman Fellowship, National Nanofabrication Users Network, the Camille Henry-Dreyfus Foundation, and the American Chemical Society.

Note added.—After submission of this manuscript, Ugawa *et al.* [23] reported an infrared study of bulk SWNT samples suggesting the existence of small-gap semiconducting SWNTs in laser ablation materials. The authors did not perform transport measurements to elucidate the electrical properties of the small-gap nanotubes.

-
- [1] M.S. Dresselhaus, G. Dresselhaus, and P.C. Ecklund, *Science of Fullerenes and Carbon Nanotubes* (Academic Press, San Diego, 1996).
- [2] R. Saito, M. Fujita, G. Dresselhaus, and M. S. Dresselhaus, *Appl. Phys. Lett.* **60**, 2204 (1992).
- [3] N. Hamada, S. Sawada, and A. Oshiyama, *Phys. Rev. Lett.* **68**, 1579 (1992).
- [4] C. T. White, D. H. Robertson, and J. W. Mintmire, in *Clusters and Nanostructured Materials*, edited by P. Jena and S. Behera (Nova, New York, 1996), p. 231.
- [5] X. Blase, L. X. Benedict, E. L. Shirley, and S. G. Louie, *Phys. Rev. Lett.* **72**, 1878 (1994).
- [6] C. L. Kane and E. J. Mele, *Phys. Rev. Lett.* **78**, 1932 (1997).
- [7] S. J. Tans, M. H. Devoret, H. Dai, A. Thess, R. E. Smalley, L. J. Geerligs, and C. Dekker, *Nature (London)* **386**, 474 (1997).
- [8] M. Bockrath, D. H. Cobden, P. L. McEuen, N. G. Chopra, A. Zettl, A. Thess, and R. E. Smalley, *Science* **275**, 1922 (1997).
- [9] S. Tans, A. Verschueren, and C. Dekker, *Nature (London)* **393**, 49 (1998).
- [10] R. Martel, T. Schmidt, H. R. Shea, T. Hertel, and P. Avouris, *Appl. Phys. Lett.* **73**, 2447 (1998).
- [11] H. Soh, C. Quate, A. Morpurgo, C. Marcus, J. Kong, and H. Dai, *Appl. Phys. Lett.* **75**, 627 (1999).
- [12] J. Kong, C. Zhou, A. Morpurgo, T. Soh, C. Marcus, C. Quate, and H. Dai, *Appl. Phys. A* **69**, 305 (1999).
- [13] J. Nygard, D. H. Cobden, M. Bockrath, P. L. McEuen, and P. E. Lindelof, *Appl. Phys. A* **69**, 297 (1999).
- [14] T. Odom, J. Huang, P. Kim, and C. M. Lieber, *Nature (London)* **391**, 62 (1998).
- [15] J. W. G. Wildoer, L. C. Venema, A. G. Rinzler, R. E. Smalley, and C. Dekker, *Nature (London)* **391**, 59 (1998).
- [16] J. Kong, H. Soh, A. Cassell, C. F. Quate, and H. Dai, *Nature (London)* **395**, 878 (1998).
- [17] The gate efficiency factor α for our general sample geometry can be estimated by using Coulomb blockade theory on our high resistance (hundreds of kiloOhms) metallic SWNT samples that exhibit periodic Coulomb oscillations in conductance vs gate voltage measurements. The typical oscillation period is $\Delta V_g \sim 200$ meV. From the previously found Coulomb charging energy $U \sim 1.4$ eV/L (nm), energy level spacing $\Delta E \sim 0.5$ eV/L [8], and $L \sim 3$ μ m, we obtain $\alpha \approx (\Delta E + U)/\Delta V_g \sim 2.5$ meV/V.
- [18] The SGS-SWNT sample described in this Letter was highly stable and allowed for reproducible transport data. Nevertheless, upon repeated thermal cycles and loading/unloading the sample, shift in V_g^* by several volts was observed. This indicates slightly different environments felt by the nanotube during different cooling cycles. Results shown in Fig. 2 were recorded during a different thermal cycle from that shown in Figs. 1 and 3. A shift in V_g^* had occurred.
- [19] C. L. Kane, E. J. Mele, R. Lee, J. E. Fischer, P. Petit, H. Dai, A. Thess, R. E. Smalley, A. R. M. Verschueren, S. J. Tans, and C. Dekker, *Eur. Phys. Lett.* **6**, 683 (1998).
- [20] C. Zhou, J. Kong, and H. Dai (to be published).
- [21] J. Nygard, D. Cobden, M. Bockrath, P. McEuen, and P. Lindelof, *Appl. Phys. A* **69**, 297 (1999).
- [22] C. Schonenberger, A. Bachtold, C. Strunk, and J. Salvétat, *Appl. Phys. A* **69**, 283 (1999).
- [23] A. Ugawa, A. Rinzler, and D. Tanner, *Phys. Rev. B* **60**, R11 305 (1999).